Transportation Research Part D 18 (2013) 122–130

Contents lists available at SciVerse ScienceDirect

Transportation Research Part D

journal homepage: www.elsevier.com/locate/trd

Investigation on lowering commuters' in-cabin exposure to ultrafine particles

Bin Xu [a], Yifang Zhu [b,*]

[a] Department of Environmental Engineering, Tongji University, 1239 Siping Road, 200092 Shanghai, China
[b] Department of Environmental Health Sciences, University of California Los Angeles, 650 Charles E. Young Drive S., Los Angeles, CA 90095, USA

ARTICLE INFO

Keywords:
Ultrafine particles
Vehicular emissions
In-cabin emissions
Driving conditions

ABSTRACT

To determine ways to reduce commuters' ultrafine particle exposure, factors such as ventilation condition, mechanical airflow rate, driving speed, cabin air filter quality, and cabin air filter use are examined. The results show that the in-cabin to on-roadway ratio is reduced by 20% when the fan is set to recirculation-on versus when set to recirculation-off because fewer ultrafine particles are exchanged between the inside and outside of the cabin. Also, when the fan is set to recirculation-off, the ratio is reduced by 40% at lower mechanical airflow rates. The thickest cabin air filter resulted in a 30% in-cabin to on-roadway ratio decrease compared with the thinnest. Thus, driving conditions with the least UFP in-cabin to on-roadway ratio is when a vehicle is operating with a high efficiency cabin filter, the ventilation set to fan-on and recycling is recirculation on, and at a high ventilation airflow rate. Furthermore, recirculating in-cabin air through a high efficiency particulate air filter was found to significantly reduce in-cabin UFP exposure.

1. Introduction

On-roadway concentrations and in-cabin to on-roadway (I/O) concentration ratios are two factors that determine a commuter's exposure to vehicle-emitted ultrafine particles (UFPs) inside cars. In general, on-roadway UFP concentrations are determined by emissions from all the surrounding vehicles and thus, are beyond the control of an individual commuter. Car commuters do, however, have some control over their exposure through modifying such things as ventilation settings. Here, to examine the impact of such options on I/O ratio, we use developed models that incorporate major physical processes of UFP transport and transformation from on-roadway to in-cabin, such as penetration across vehicle cracks, filtration through the cabin filters, and deposition inside the vehicles, paying particular attention to the ventilation settings.

2. Methods

The I/O UFP ratio is directly affected by a variety of driving conditions. To investigate the effect of driving conditions on the ratio, Xu and Zhu's (2009) model is developed. UFP transport and transformation of exposure from on-roadway to in-cabin is described on a material-balance basis, as shown in the following equation:

$$\frac{d(C_i V)}{dt} = C_0[Q_S(1-\eta_S) + Q_L P] - C_i[Q_F \eta_F + \beta V + (Q_S + Q_L)] \quad (1)$$

* Corresponding author.
E-mail address: yifang@ucla.edu (Y. Zhu).

1361-9209/$ - see front matter © 2012 Elsevier Ltd. All rights reserved.
http://dx.doi.org/10.1016/j.trd.2012.10.005

Outdoor UFPs can enter the in-cabin microenvironment through the mechanical air supply at a flow rate of Q_S ($m^3\ h^{-1}$) and at a leakage flow rate of Q_L ($m^3\ h^{-1}$). For a particular particle size, d, the in-cabin particle concentration is C_i (particles cm^{-3}), the on-roadway concentration is C_0 (particles cm^{-3}), and V (m^3) is the volume of the vehicle's interior. The variables, P, η_S, η_F, and β, are the penetration factor, filtration efficiency, removal fraction by respiratory, and deposition coefficient (h^{-1}). Among the in-cabin UFP dynamics, Q_S, V, P, η_S, and β have been determined experimentally by Gong et al. (2009), Xu et al. (2010, 2011), and Q_L can be calculated theoretically (Baker et al., 1987).

This model, however, needs to be adjusted under ventilation condition of whether the air recirculation (RC) is on or off. With the air conditioning fan on, the in-cabin air pressure is usually greater than the outside pressure, which leads to an in-cabin UFP loss. The in-cabin UFP dynamic model is thus revised to allow for RC to be off but the fan on:

$$\frac{d(C_i V)}{dt} = C_0[Q_S(1-\eta_S)] - C_i[Q_F\eta_F + Q_L P + \beta V + (Q_S + Q_L)] \tag{2}$$

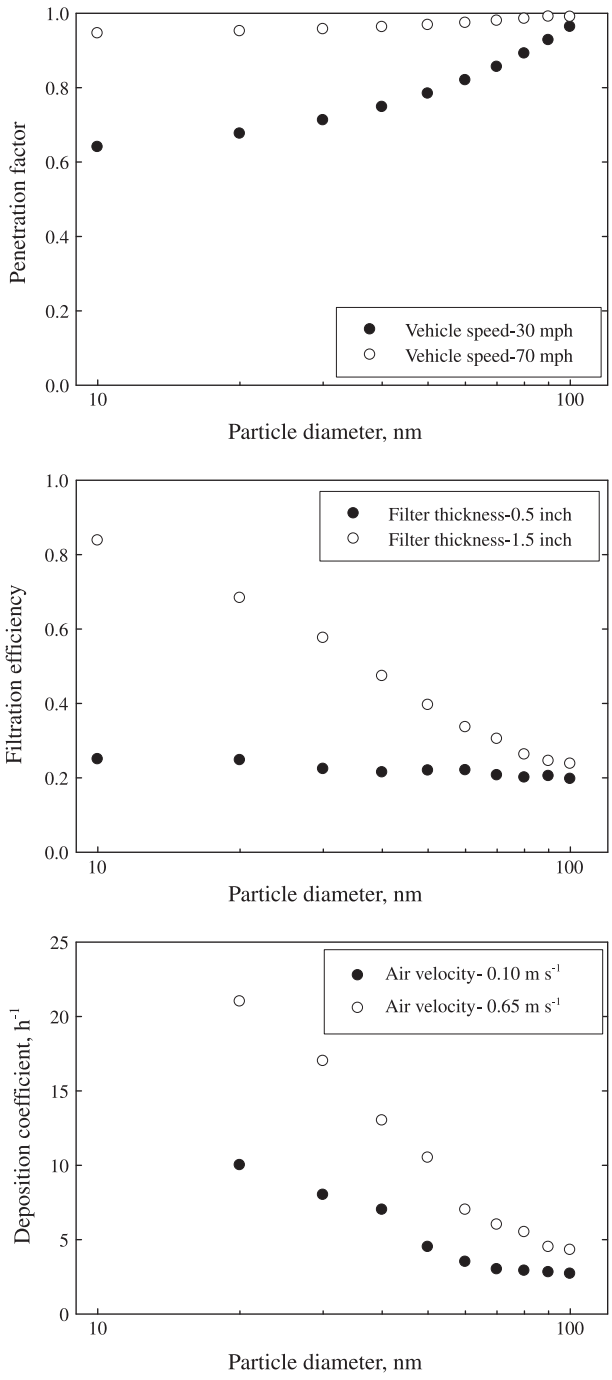

Fig. 1. Size-segregated parameters governing in-cabin UFP transport and transformation dynamics.

Fig. 1 illustrates the range of size-segregated important parameters that affects the movements of UFP and the transformation from on-roadway to in-cabin. The fraction of particles passing the vehicle envelope through the leakage airflow is defined by a penetration factor, P. This parameter is measured at various crack sizes on the vehicle envelope under various pressure drops across the cracks at various speeds between 30 and 70 mph. The largest found at the highest pressure drop (200 Pa), and the smallest at the lowest (30 Pa). η_S is determined by measuring commercially-available cabin filters with thicknesses of 1.5, 1, and 0.5 in. over a range of filter face velocities (0.1–0.5 m s^{-1}) that are equipped in 1997 Isuzu Rodeo, 2000 Nissan Altima, and 2005 Ford F-150 passenger vehicles. The filtration efficiency varies significantly with respect to filter thicknesses (Fig. 1b). β is measured in the 1996 Saturn SL2, 1997 Isuzu Rodeo, and 2005 Ford F-150 with in-cabin air velocities (0–0.65 m s^{-1}) measured at the ventilation setting, fan-off, recirculation-off; fan-on, recirculation-off; fan-on, recirculation-on. The highest deposition coefficient occurred at the highest in-cabin air velocity (Fig. 1c).

Under ventilation combinations (i) fan-off, recirculation-off; (ii) fan-on, recirculation-off; and (iii) fan-on, recirculation-on, Eq. (1) can be simplified with respect to UFP entry pathways from the on-roadway atmosphere to the in-cabin environment. For example, under condition (i), there is no mechanical air supply ($Q_S = 0$), and Eq. (1) reduces to, $\frac{C_i}{C_0} = \frac{Q_L P}{Q_F \eta_F + \beta V + Q_L}$ indicating that commuters can lower the UFP I/O ratio by minimizing P and Q_L. Similarly, under condition (ii), Eq. (2) is reduced to: $\frac{C_i}{C_0} = \frac{Q_S(1-\eta_S)}{Q_F \eta_F + Q_L P + \beta V + Q_S + Q_L}$, whereby the UFP I/O ratio can be reduced by decreasing Q_S and increasing η_S; under condition (iii), the UFP I/O ratio can be reduced by decreasing P and Q_L.

The parameters that govern the in-cabin UFP dynamics are all related to vehicles' cabin environments, of which ventilation combinations, ventilation airflow rate, driving speed, and cabin filter usage can be controlled, at least to a degree, by the commuters.

3. Results

3.1. Ventilation condition

Fig. 2 shows UFP I/O ratios as a function of particle size under the various ventilation conditions calculated by introducing the penetration factor, filtration efficiency and deposition coefficient, shown in Fig. 1. Under conditions (i and iii), the greatest I/O ratios are found corresponding to the highest penetration factor and lowest filtration efficiency, and deposition coefficients. Regarding condition (ii), the largest I/O ratio is found at the smallest penetration factor and lowest filtration efficiency. The largest penetration factor is related to the largest driving speed, largest crack height, and shortest crack length. As one would expect, the lowest filtration efficiency is with the thinnest filter at the lowest filter face velocity. The lowest deposition coefficient occurs inside vehicles with the smallest interior surface to volume ratio and at the lowest in-cabin air velocity. In general, this condition reflects driving an old, leaky, large vehicle with a poor quality in-cabin filter at high speed.

The greatest variability in the I/O ratio, about 40%, occurs with smaller particle sizes under (ii) because of the large difference in filtration efficiencies with respect to filter thicknesses (Fig. 2b). Among the ventilation combinations, up to 20% variability in median I/O ratios are found. The average highest and lowest I/O ratios are under conditions (ii and iii). In addition, although the I/O trends as a function of particle size are similar for all three ventilation combinations, the underlying mechanisms resulting in each trend are different. With (i), the I/O ratios increased with increasing particle size due to the larger penetration factor for larger particles that leads to more particle entry through leakage. For condition (ii), the I/O ratios increased with increasing particle size due to the lower filtration efficiency for larger particles and the larger penetration factor that leads to more particle exit through leakage. For condition (iii), the I/O ratios increased with increasing particle size due to the larger penetration factor and the smaller deposition coefficient for larger particles.

Under condition (i), the leakage airflow is the predominant pathway for air and UFP exchange between the in-cabin and the outside. It is found that the penetration factors and the leakage rate are the most important parameters that affect the UFP I/O ratios under this ventilation setting. Under (ii), the mechanical airflow is the dominant air exchange process for the in-cabin microenvironment. The air exchange rate is larger under condition (ii) than (i and iii) because the mechanical airflow has a greater effect than the leakage flow (Xu and Zhu, 2009), which leads to the largest median I/O UFP ratio, as shown in Fig. 2. Under condition (iii), the in-cabin air is re-circulated, and the leakage airflow becomes the predominant pathway for air and UFP exchange between the in-cabin and on-roadway atmosphere. When the ventilation setting is switched from condition (i) to condition (iii), the in-cabin air velocity increased, which enhanced the UFP deposition on the vehicle interior surfaces and resulted in a lower median I/O UFP ratio. As shown in Fig. 2, the median UFP I/O ratio is the lowest with (iii), which is consistent with the previous in-cabin UFP I/O ratio measurement during freeway and tunnel travel (Zhu et al., 2007; Knibbs et al., 2010). Therefore, to minimize the in-cabin UFP levels, it is recommended that commuters set ventilation combinations to fan-on, recycling-on. However, it should be noted that under this ventilation condition, there is a minimal air exchange between the in-cabin and the outside, which results in a quick build-up of in-cabin CO_2 levels.

3.2. Mechanical ventilation airflow rate

Besides the ventilation conditions, the mechanical ventilation airflow rate also significantly affects the UFP I/O ratio. Fig. 3 presents the UFP I/O ratios as a function of the mechanical airflow rate in the range of 0–360 m^3 h^{-1}. The I/O ratio

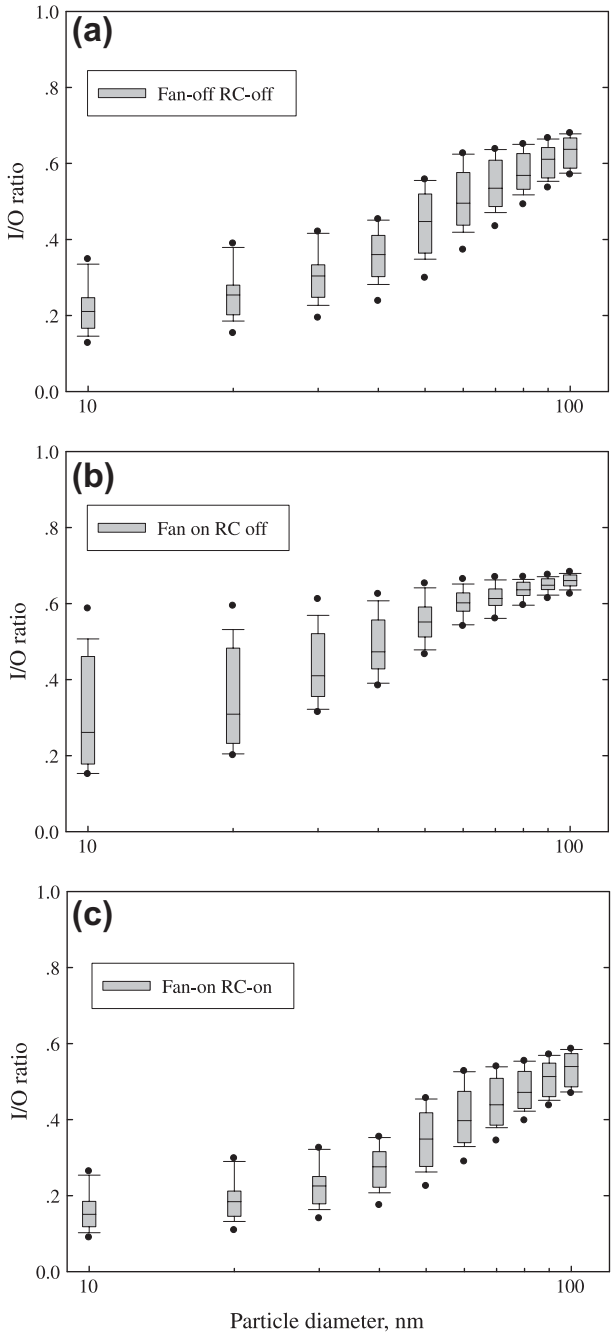

Fig. 2. The range of *I*/*O* ratios under various ventilation settings. *Note*: volume of the vehicle is 6 m^3.

significantly increased under condition (ii), where the mechanical air supply is the predominant airflow and thus, determined the in-cabin air exchange rate. The mechanical airflow rate and filtration efficiency are covariant: the faster the airflow passed through, the lower the filtration efficiency. The larger air exchange rate and the lower filtration efficiency can both result in more UFPs entering into vehicle cabins, which can lead to an increased *I*/*O* ratio. In contrast, the *I*/*O* ratio is reduced under condition (iii). The increased in-cabin air velocity led to larger deposition coefficients for all UFP sizes (Gong et al., 2009). More UFPs deposited on the vehicle interior surface results in a lower *I*/*O* ratio. Therefore, under (ii), a lower ventilation airflow rate should be chosen by commuters to achieve a lower in-cabin UFP exposure.

3.3. Driving speed

In addition to the ventilation settings and the airflow rate, vehicle driving speed also significantly affects the UFP *I*/*O* ratio. In an earlier study, it is found that a larger driving speed created a larger pressure differential between the in-cabin and the outside that resulted in larger leakage airflow (Ott et al., 2007), greater air exchange rate (Fruin et al., 2011) and greater

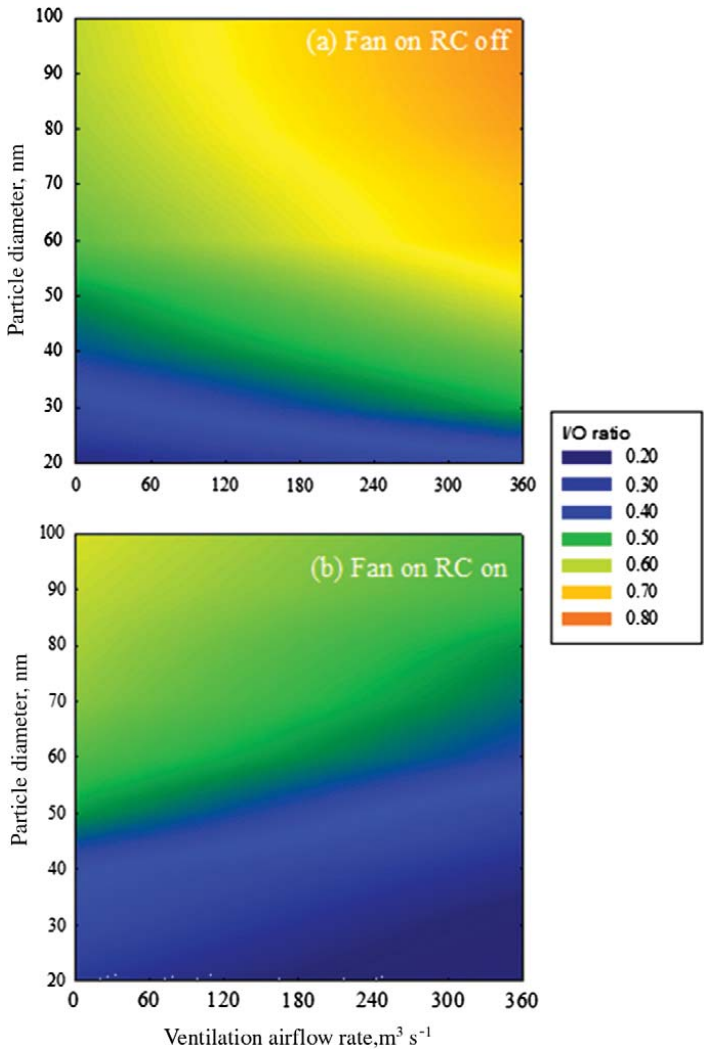

Fig. 3. The range of the *I*/*O* ratios at different mechanical air flow rates under two ventilation settings. *Note*: The volume of vehicle is 6 m^3, and the speed of vehicle is 50 mph.

particle penetration (Xu et al., 2010). The pressure differential between the in-cabin and the outside allows the leakage airflow to bring UFPs into the vehicle under combinations (i and iii) but pull UFPs out of the vehicle under condition (ii) through cracks in the vehicle envelope. Both the leakage airflow rate and the penetration factor are significantly affected by the pressure differential between the in-cabin and the outside. Previously, Xu and Zhu (2009) found that the pressure differential increased from 30 ± 5 Pa to 150 ± 40 Pa when a vehicle's speed increases from 30 mph to 70 mph under various ventilation settings.

Fig. 4 illustrates the relationship between UFP *I*/*O* ratios and vehicle driving speeds for UFP sizes (10–100 nm). For ventilation combinations (i and iii), at a given vehicle speed, the differential pressures between the outside and the in-cabin are the same resulting in the same amount of leakage airflow. A larger penetration factor of the larger particles resulted in more particles leaking into the vehicle.

The *I*/*O* ratios are largest at the fastest driving speed. A faster driving speed leads to more UFP penetration, which results in higher *I*/*O* ratios. However, the relative importance of the vehicle speed changes with different ventilation settings. Compared with condition (ii), the vehicle speed is more significant under (i and iii). The vehicle driving speed directly affects the differential pressure between the in-cabin and the outside, which determines the leakage airflow rate. When there is no mechanical ventilation air supply from the on-roadway atmosphere into the in-cabin (conditions (i and iii)), the UFPs penetration is predominantly caused by leakage into the in-cabin and results in a greater increase of the *I*/*O* ratio. In contrast, when there is mechanical airflow from outside into the cabin under (ii), the in-cabin air pressure is larger than outside air pressure. The vehicle speed does not significantly affect the *I*/*O* ratio. Because a larger *I*/*O* ratio is related to a faster driving speed under ventilation combinations (i and iii), a lower driving speed achieves a lower in-cabin UFP *I*/*O* ratio.

Besides on-roadway UFP level and *I*/*O* ratio, commuting time is another parameter that determines commuters' exposure to UFP inside vehicles. The UFP exposure, denoted as *M* (particle cm^{-3} h), during commuting can be calculated as

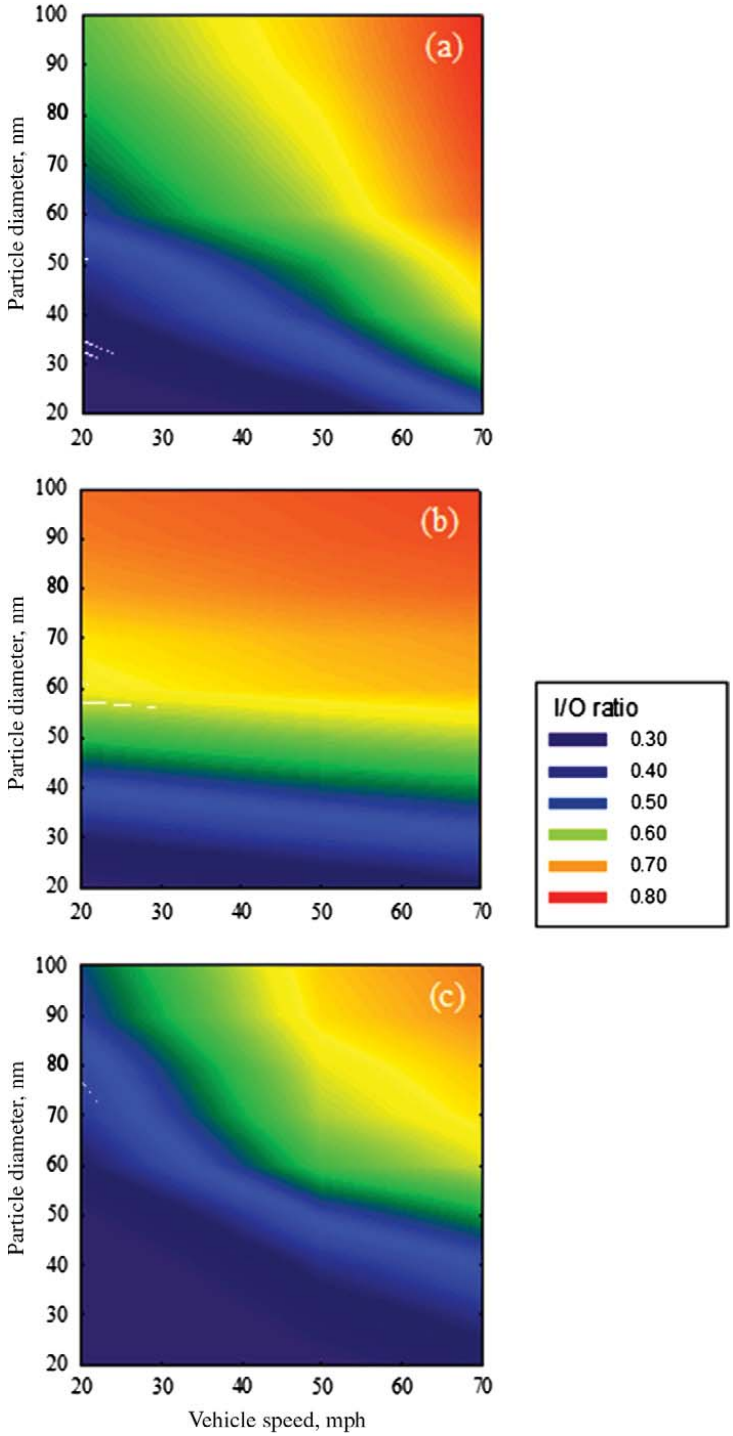

Fig. 4. The range of the *I*/*O* ratios at different vehicle speeds under three ventilation settings. *Note*: the volume of the vehicle is 6 m^3, and the ventilation airflow rate is 180 $m^3\ h^{-1}$.

$M = C \times y \times t$, where C is the on-roadway UFP concentration, y is UFP *I*/*O* ratio, and t is commuting time. For a given distance, assuming a constant on-roadway UFP concentration, the exposure will be determined by the product of y and t that both are related to vehicle speed. To achieve an explicit relationship between M and vehicle speed, Fig. 5 shows the quantitative relationship between UFP *I*/*O* ratio and vehicle speed. Linear relationships are observed under all three ventilation combinations. Similar to Fig. 4, the effect of speed on UFP *I*/*O* ratio under condition (ii) is less significant than those under (i and iii) due to the mechanical air supply through the ventilation system under the latter. The linear regression equations in Fig. 5 can then be applied to derive a quantitative relationship between UFP exposure, M and vehicle speed, x ($m\ s^{-1}$). Under condition (i), for example, $M = C \times (0.005x + 0.34) \times \frac{L}{x} = 0.005CL + \frac{0.34CL}{x}$ where L is the distance the vehicle traveled in miles. Faster driv-

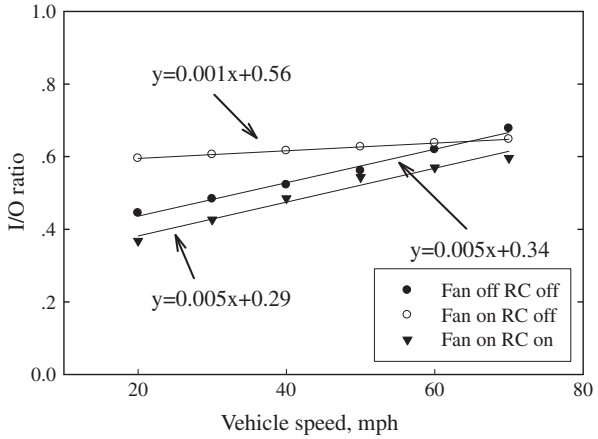

Fig. 5. Relationship between UFP I/O ratios and vehicle speeds under three ventilation settings. *Note*: ventilation airflow rate is 180 $m^3\ h^{-1}$.

ing speeds result in lower in-cabin UFP exposure levels. Similar equations can be derived under the other two combinations. Quantitatively, it takes 0.7 and 0.2 h at 20 and 70 mph, to commute 14 miles. By assuming an on-roadway UFP concentration of 10^5 particle cm^{-3}, the accumulative in-cabin exposure levels are 3.08×10^4 particle cm^{-3} h and 1.38×10^4 particle cm^{-3} h at 20 mph and 70 mph. On-roadway UFP concentrations are also likely be affected by vehicle speed. Current motor vehicle emission models (e.g., MOVES), however, do not address UFP emissions, and we do not examine the impact of vehicle speed on on-roadway UFP concentrations and in-cabin UFP exposures.

3.4. Cabin filter quality and usage

Modern vehicles are generally equipped with air filters that may reduce in-cabin UFP concentrations (Pui et al., 2008). In Xu et al. (2011), a range of filtration efficiencies (up to 60%, Fig. 1b) are found for commercial cabin air filters, where the greatest filtration efficiency occurred for the thickest commercially available cabin filter. Due to the variability in the filtration efficiency, the UFP *I*/*O* ratios can vary greatly depending on the quality of the cabin filter. Fig. 6 shows the UFP *I*/*O* ratios with cabin filters under condition (ii) when the ventilation airflow dominates the air exchange between the in-cabin and the outside (Xu and Zhu, 2009). Under condition (ii), the majority of the UFPs enter the in-cabin through the ventilation system, the large variability in filtration efficiencies results in significantly different UFP *I*/*O* ratios. With the thickest filter, the average UFP *I*/*O* ratio for the different size ranges is about 50%, and with the thinnest and worst quality filter, the average UFP *I*/*O* ratio increased to ~75%. Replacing an existing commercial cabin air filter with a high efficiency particulate air (HEPA) filter can significantly lower the in-cabin UFP exposure. The filtration efficiency of a HEPA filter is greater than 99.97% in the UFP size range (Schroth, 1996), which effectively reduces the amount of UFPs entering the in-cabin though the ventilation system. As seen in Fig. 6, the mean UFP *I*/*O* ratio decreased by 50%, with the largest reduction occurred for larger UFPs.

Filter usage also affects the UFP *I*/*O* ratios and can be controlled by commuters. Both the filtration efficiency and pressure drop across the filter increase for prolonged filter usage. Increased filtration efficiency reduces the UFP *I*/*O* ratios under fan-on, recirculation-off (Xu and Zhu, 2009). However, how the pressure drop affects the UFP *I*/*O* ratios is more complicated

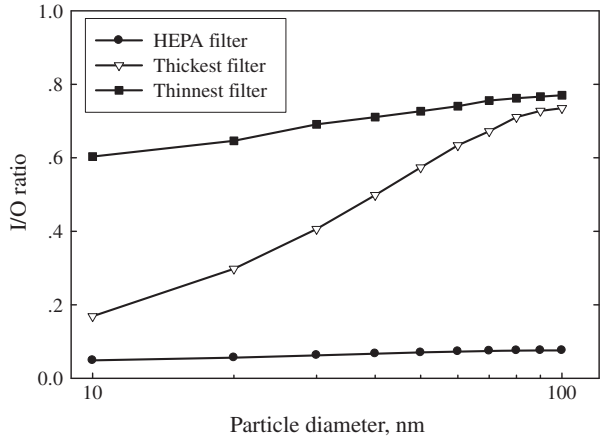

Fig. 6. The range of the *I*/*O* ratios with different filter qualities under the ventilation setting of fan-on, recycling-off. *Note*: the thickness of thickest filter and thinnest filter are 1.5 in. and 0.5 in. The ventilation airflow rate is 180 $m^3\ h^{-1}$.

because the pressure drop not only decreases the mechanical flow rate through the ventilation system but also affects the pressure differential between the in-cabin and the outside, which affects the UFP penetration. The results show that an increased differential pressure pushes more UFPs into the in-cabin through leakage, which results in a higher I/O ratio.

The effect of the filter usage on the I/O ratio also depends on traffic. For the same filter usage, the results showed that heavy traffic accelerated the particle loading on the filter, which resulted in a larger pressure drop across the filter and a greater UFP I/O ratio compared with when under light traffic. Fig. 7 shows the UFP I/O ratios as a function of filter usage at a condition of moderate traffic with the fan-on and recirculation-off. The I/O ratio increased nearly 20% over 30 months of filter usage.

3.5. Recirculation air passing through a HEPA cabin air filter

Other vehicle models, especially newer ones have recalculating air go through the cabin air filter that may result in a substantial in-cabin UFP reduction. Under these conditions, no UFPs would be transported by the mechanical ventilation air from the on-roadway atmosphere. In addition to deposition, if the in-cabin UFPs are removed by the cabin air filter at a rate of $Q_S\eta_S$, then Eq. (1) can be modified to Eq. (2).

$$\frac{d(C_iV)}{dt} = C_0Q_LP - C_i(Q_F\eta_F + \beta V + Q_S\eta_S + Q_L) \tag{3}$$

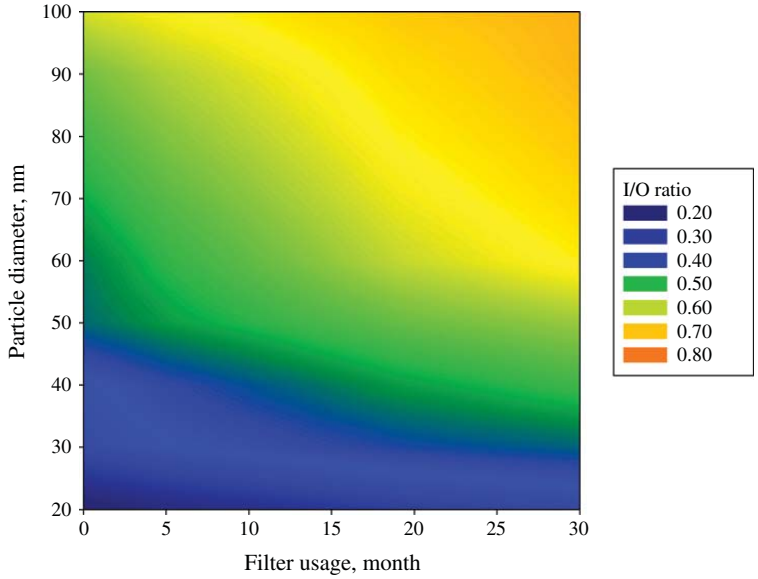

Fig. 7. Modeled UFP I/O ratios as a function of filter usage. *Note*: the best quality filter are used in the calculations. The volume of the vehicle is 6 m^3, and the ventilation airflow rate, 180 $m^3\ h^{-1}$.

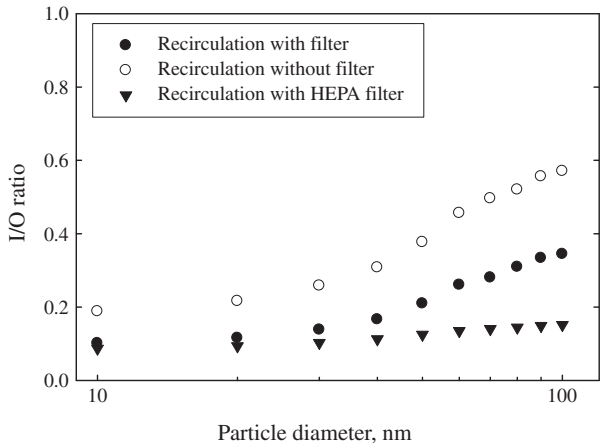

Fig. 8. The range of I/O ratios under various ventilation settings. *Note*: the ventilation airflow rate is 180 $m^3\ h^{-1}$.

At steady-state, the UFP I/O ratio is $\frac{C_i}{C_0} = \frac{Q_L P}{Q_F \eta_F + \beta V + Q_S \eta_S + Q_L}$. Fig. 8 shows the UFP I/O ratios as a function of particle size under condition (iii) with and without recirculation air passing through the cabin air filter. When the recirculating air does not pass through the cabin air filter, the average UFP I/O ratio is 30% in the UFP size range. The UFP I/O ratio decreased 10–30% when the recirculating air passed through the cabin air filter in the ventilation system. The lowest I/O ratio is when the recirculating air passed through a HEPA filter. The I/O ratio through the UFP size range is lower than 15%.

4. Conclusions

With regard to the effects of ventilation settings, and driving conditions on the UFP in-cabin to on-roadway concentration ratios, the latter are found to vary significantly under different ventilation settings and driving conditions. From an environmental health perspective, commuters are advised to drive at the speed limit using the largest ventilation airflow rate with the fan-on and recirculation-on and to use a high-efficiency cabin filter to reduce exposure to in-cabin UFPs. Recirculating in-cabin air through a HEPA filter is also found to greatly reduce in-cabin UFP exposures.

Acknowledgments

This study was supported by the Walter A. Rosenblith New Investigator Award from the Health Effects Institute under Contract # 4764-FRA06-3107-5 and the National Science Foundation's CAREER Award under Contract # 32525-A6010. Bin Xu acknowledges support from the National Nature Science Foundation of China (Grant No. 51208372).

References

Baker, P., Sharples, S., Ward, I., 1987. Air-flow through cracks. Building and Environment 22, 293–304.
Fruin, S., Hudda, N., Sioutas, C., Delfino, R., 2011. Predictive model for vehicle air exchange rates based on a large representative sample. Environmental Science and Technology 45, 3569–3575.
Gong, L., Xu, B., Zhu, Y., 2009. Ultrafine particles deposition inside passenger vehicles. Aerosol Science and Technology 43, 544–553.
Knibbs, L., De Dear, R., Morawska, L., 2010. Effect of cabin ventilation rate on ultrafine particle exposure inside automobiles. Environmental Science and Technology 44, 3546–3551.
Ott, W., Klepeis, N., Switzer, P., 2007. Air change rates of motor vehicles and in-vehicle pollutant concentrations from secondhand smoke. Journal of Exposure Science and Environmental Epidemiology 17, 1–14.
Pui, D., Qi, C., Stanley, N., Oberdorster, G., Maynard, A., 2008. Recirculating air filtration significantly reduces exposure to airborne nanoparticles. Environmental Health Perspectives 116, 863–866.
Schroth, T., 1996. New HEPA/ULPA filters for clean-room technology. Filtration & Separation 33, 245–250.
Xu, B., Zhu, Y., 2009. Quantitative analysis of the parameters affecting in-cabin to on-roadway (I/O) ultrafine particle concentration ratios. Aerosol Science and Technology 43, 400–410.
Xu, B., Liu, S., Zhu, Y., 2010. Ultrafine particle penetration through idealized vehicle cracks. Journal of Aerosol Science 41, 859–868.
Xu, B., Liu, S., Liu, J., Zhu, Y., 2011. Effects of cabin filter on in-cabin to on-roadway ultrafine particle ratios. Aerosol Science and Technology 45, 215–224.
Zhu, Y., Eiguren-Fernandez, A., Hinds, W., Miguel, A., 2007. In-cabin commuter exposure to ultrafine particles on Los Angeles freeways. Environmental Science and Technology 41, 2138–2145.